Geometry of Laser Spot Welds from Dimensionless Numbers

A. ROBERT and T. DEBROY

Recent computer calculations of heat transfer and fluid flow in welding were intended to provide useful insight about weldment geometry for certain specific welding conditions and alloys joined. However, no generally applicable correlation for the joining of all materials under various welding conditions was sought in previous work. To address this difficulty, computer models of fluid flow and heat transfer were used for the prediction of weld pool geometry in materials with diverse properties, such as gallium, pure aluminum, aluminum alloy 5182, pure iron, steel, titanium, and sodium nitrate under various welding conditions. From the results, a generally applicable relationship was developed between Peclet (Pe) and Marangoni (Ma) numbers. For a given material, Ma and Pe increased with the increase in laser power and decrease in beam radius. For materials with high Prandtl number (Pr), such as sodium nitrate, the Pe and Ma were high, and heat was transported primarily by convection within the weld pool. The resulting welds were shallow and wide. For low Pr number materials, like aluminum, the Pe and Ma were low in most cases, and low Pe made the weld pool deep and narrow. The cross-sectional areas of stationary and low speed welds could be correlated with welding conditions and material properties using dimensionless numbers proposed in this article.

I. INTRODUCTION

IN the past twenty years, significant progress has been made in understanding the evolution of weld pool geometry based on experiments and computer modeling.[1±6] Computer simulation efforts have largely focused on numerical calculations of heat transfer, fluid flow, and their effects on the shape and size of the weld pool. These efforts have resulted in significant findings that are valid, in most cases, for a combination of specific welding conditions and the alloy system investigated in each case. As a result, previous research remains disjointed as evidenced by lack of general correlations that are useful in various welding conditions and welded materials.

The literature on heat transfer and fluid flow calculations in welding to obtain generally useful dimensionless correlations among important variables is scarce. Chan *et al.*[1,2] discussed the effect of dimensionless numbers on the shape of the weld pool using two- and three-dimensional models of the fluid flow and heat transfer in a laser melted pool for different materials. The focus was to examine the effects of several selected dimensionless numbers on the computed temperature and velocity fields. Recently Limmaneevichitir and Kou[7] tried to explain the shape of the weld pool based on Prandtl number (Pr) for different materials by conducting laser-welding experiments with gallium and $NaNO_3$, but no general correlation among dimensionless numbers was sought. Mendez and Eager[8] used a nondimensional system of equations for arc welding to explain the fingerlike penetration and hump bead formation, but this study was focused on high current and high welding speed. Fuerschbach[9,10] developed a dimensionless parameter model for linear laser and arc welds for the prediction of cross-sectional area considering the physical properties of the welded material and the welding parameters. The results were applicable to moving linear welds since the correlation required welding velocity. Currently, no correlation is available for the prediction of weld pool size or geometry of stationary laser welds in terms of dimensionless numbers.

Cross sections of stationary laser welds for various materials under different welding conditions are shown[7,11,12] in Figure 1. Widely different shapes and sizes of the weld pools can be observed for various materials under different welding conditions. Gallium and aluminum alloy 5182 weld pools are narrow and deep with high aspect ratios (0.32 to 0.5), which is defined as the ratio of weld pool depth to width. The gallium weld pool has nearly hemispherical shape and the aluminum alloy 5182 exhibits a concave weld pool bottom. Steel welds are shallow with low aspect ratios (<0.3). Steel weld with higher laser power has a relatively flat bottom. Laser-treated $NaNO_3$ weld pools are wide and shallow with very low aspect ratios (0.1 to 0.18). These weld pools exhibit a very peculiar shape with a deep pool near the periphery and shallow depth at the middle of the weld pool. At present, no theory exists to understand either the cross-sectional area or the various fusion zone shapes observed in stationary laser welds of different materials for different welding conditions. The goal of this research is to seek correlations among dimensionless numbers aimed at understanding different shapes of weld pools and predicting weld cross-sectional area in stationary and low speed conduction mode laser welds of various materials that do not contain any surface active elements. By comparing experimentally-determined and numerically-computed weld pool geometry in gallium, pure aluminum, aluminum alloy 5182, pure iron, steel, titanium, and sodium nitrate, we seek to understand different fusion zone geometry in welds of different materials under various welding conditions.

II. APPROACH

Two-[12] and three-dimensional[13] computational models of heat transfer and fluid flow in the weld pool were used

A. ROBERT, Graduate Student, and T. DEBROY, Professor, are with the Department of Materials Science and Engineering, The Pennsylvania State University, University Park, PA 16802.

Manuscript submitted November 7, 2000.

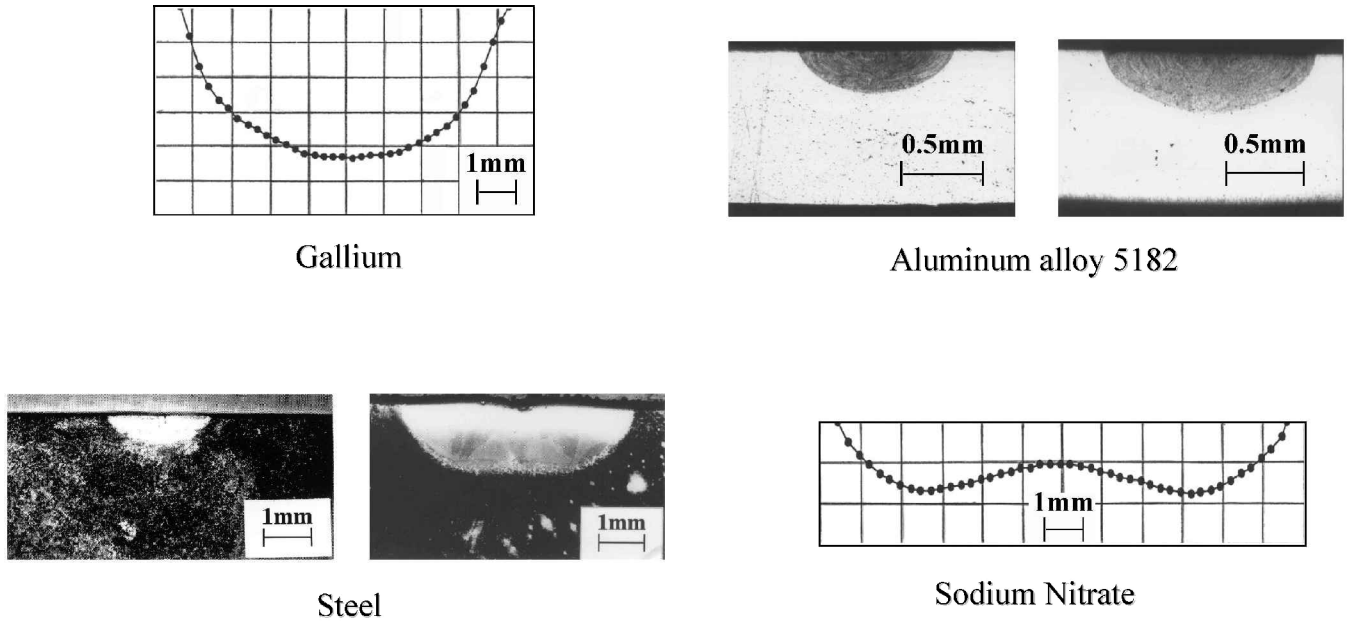

Fig. 1–Geometry of stationary laser welds for different materials and welding conditions. [7,11,12]

for the prediction of weld pool geometry in gallium, pure aluminum, aluminum alloy 5182, pure iron, steel, titanium, and sodium nitrate under different welding conditions. The predicted weld pool geometry for various materials under different welding conditions was compared with independent experimental results. The comprehensive information obtained from the verified phenomenological model was used to develop generalized correlations in terms of dimensionless numbers.

The physical properties of different materials considered in the present study are shown in Table I. The welding conditions for various materials considered in this study are presented in Table II. A wide range of Pr numbers, which is the ratio of momentum diffusivity to thermal diffusivity ($= \nu/\alpha$, where ν is kinematic viscosity or momentum diffusivity, and α is thermal diffusivity), was considered for the study. The values of Pr ranged from 0.012 for aluminum to 9.15 for $NaNO_3$. Thus, the Pr numbers studied covered the entire range of commonly welded alloys.

III. RESULTS AND DISCUSSION

The computed and experimental weld pool geometry for different materials are shown in Figures 2 through 5. It can be observed that the computer model predictions of weld pool geometry are in good agreement with the corresponding experimentally-observed values in all cases. Different weld pool geometry was obtained depending on the welding conditions and the material properties. The relative magnitude of heat transported by convection and conduction in the weld pool affects its shape. If convection is the primary mechanism of heat transfer from the middle to the edge of the weld pool, the weld pool becomes wide. As a result, the aspect ratio of the pool becomes small. On the other hand, when heat is transported primarily by conduction, heat diffuses away from the middle of the weld pool in all directions. This makes the weld pool nearly hemispherical. The different weld pool shapes observed in Figures 2 through 5 can be described in terms of two dimensionless numbers, *i.e.*, Peclet (Pe) number and Marangoni (Ma) number.

A. *Weld Pool Shape and Dimensionless Numbers*

The dimensional analysis shows that the half width or ™radius of the weld pool, the thermal diffusivity, the temperature coefficient of the surface tension, the temperature drop from the center to the edge of the weld pool, the viscosity, and the maximum surface velocity can be expressed in terms of two dimensionless numbers, *i.e.*, Ma and Pe. The Ma number, which is the measure of intensity of surface tension driven convection, is defined as

$$\mathrm{Ma} = \frac{-\frac{d\gamma}{dT} W \Delta T}{2\mu\alpha_1} \qquad [1]$$

where W is the width of the weld pool, ΔT is the temperature drop from the center to the edge of the weld pool, $d\gamma/dT$ is the temperature coefficient of the surface tension, μ is viscosity, and α_1 ($=K_l/\rho C_{pl}$) is thermal diffusivity of liquid metal. When the input power is increased or the beam radius is decreased, the value of ΔT increases and, consequently, Ma increases. The Pe number, which is the measure of relative heat transport by convection and conduction from center to the edge of the weld pool, is defined as

$$\mathrm{Pe} = \frac{WV_{\max}}{2\alpha_1} \qquad [2]$$

where, W is the width of the weld pool, $V_{\max}$ is the calculated maximum surface velocity, α_1 is the thermal diffusivity of liquid, K_l is the thermal conductivity of liquid metal, ρ is the density, and C_{pl} is the specific heat of liquid metal.

In the absence of a surface-active element in the weld metal, the metal flows outward at the surface from the middle

Table I. Physical Properties of Different Materials Considered[7,13,14,16]

Material	ρ (kg/m^3)	μ (kg/m s)	C_{ps} (J/kg K)	C_{pl} (J/kg K)	K_s (J/m s K)	K_l (J/m s K)	α_s (m^2/s)	α_l (m^2/s)	Pr	$-d\gamma/dt$ (N/m K)	T_m (K)	H_f (J/kg)
Al	2400.0	1.1×10^{-3}	894.5	1078.5	212.3	99.9	1.0×10^{-4}	3.86×10^{-5}	0.012	3.5×10^{-4}	933.0	4.0×10^5
Al alloy 5182	2300.0	1.1×10^{-3}	898.7	1199.7	167.6	107.8	8.1×10^{-5}	3.91×10^{-5}	0.012	3.5×10^{-4}	*850/911	*7.2×10^{-4}/1.1×10^6
Ga	6100.0	1.94×10^{-3}	392.9	409.7	33.0	33.0	1.4×10^{-5}	1.32×10^{-5}	0.024	1.0×10^{-4}	302.9	8.0×10^4
Pure iron	7800.0	5.0×10^{-3}	455.6	823.5	31.3	31.3	8.8×10^{-6}	4.9×10^{-6}	0.131	5.0×10^{-4}	1811.0	2.7×10^5
High speed steel	8100.0	6.0×10^{-3}	627.0	723.2	22.9	22.9	4.5×10^{-6}	3.92×10^{-6}	0.189	5.0×10^{-4}	1620.0	2.5×10^5
Titanium	4540.0	5.0×10^{-3}	526.7	781.7	20.5	20.5	8.6×10^{-6}	5.8×10^{-6}	0.191	2.6×10^{-4}	1941.0	3.6×10^5
$NaNO_3$	1900.0	3.02×10^{-3}	1095.2	1709.6	0.564	0.564	2.7×10^{-7}	1.7×10^{-7}	9.15	5.9×10^{-5}	579.8	1.8×10^5

*For aluminum alloy 5182 solidus and liquidus temperatures and the corresponding enthalpy at these temperatures are indicated here.

to the edge of the weld pool mainly due to the spatial variation of surface tension at the weld pool surface.[12] At the weld pool surface, this flow aids in transporting heat from the middle to the edge of the pool. Therefore, in calculating dimensionless numbers, the half width or radius of the weld pool and the maximum surface velocity are taken as the characteristic length and velocity, respectively. Equation [2] indicates that when the value of Pe is much greater than 1, the rate of transport of heat by convection from the center to the periphery of the weld pool is much higher than that by conduction.

Pe and Ma were evaluated from Eqs. [1] and [2] for the experimental conditions shown in Table II. The input parameters, such as maximum temperature drop in the weld pool and maximum surface velocity at weld pool surface, were obtained from the modeling results. The relationship between Pe and Ma for various materials under different processing conditions is shown in Figure 6. The correlation between Pe and Ma can be expressed as

$$\mathrm{Pe} = 0.08\mathrm{Ma}^{0.93} \qquad [3]$$

The correlation coefficient between the data and Eq. [3] is 0.95. Large values of Ma indicate a strong driving force for convection at the weld pool surface. Under these conditions, heat is transported rapidly in the radial direction by convective heat transport and consequently, a high value of Pe is obtained.

For the welding of a given material, the welding parameters have considerable influence on the range of values of Ma and Pe. For example, when the laser power increases or the beam radius decreases, the spatial gradient of temperature on the weld pool surface increases leading to a higher Ma. The resulting higher surface velocity also results in higher values of Pe. This behavior is clearly observed in Figure 6. In addition to the welding conditions, the values of these dimensionless parameters are significantly affected by material properties. For example, both Pe and Ma depend on thermal diffusivity. Materials with high thermal diffusivities, such as aluminum and aluminum alloys, have low values of Ma and Pe. On the other hand, high values of Ma and Pe are obtained for materials with low thermal diffusivity, such as $NaNO_3$.

The values of these dimensionless numbers (Pe and Ma) have important consequences in determining weld pool shape. The thermal diffusivities of gallium (1.32×10^{-5} m^2/s) and aluminum (3.9×10^{-5} m^2/s) are very high, so relatively low values of Ma and Pe were obtained. These materials are also characterized by low values of Pr (0.012 for Al and 0.024 for Ga). When Pe is much lower than 1, heat is transported mainly by conduction. For the welding of Ga and Al, the Pe values are much lower than 1 when the average weld pool velocities are considered. As a result, nearly hemispherical weld pool shapes were obtained for gallium and aluminum as observed in Figures 2 and 3.

A word of caution about the magnitude of Pe may be in order here. In Figure 6, Pe values as high as 20 are indicated for the welding of Ga. It should be recognized that highest surface velocities were used to calculate these Pe values in this figure, since the purpose was to correlate Ma, which is a measure of convection at the surface with Pe. It is more appropriate to use an average velocity for the calculation of Pe to understand the weld pool shapes indicated in Figures 2 and 3.

Table II. Specimen Geometry and Welding Conditions[3,11,12,15,16]

Material	Composition	Specimen Geometry (mm)*	Type of Welding	Power Density Distribution	Shielding Gas and Gas Flow Rate (m^3/s)	Irradiation Time (s)	Laser Power (W)	Beam Radius (mm)	Welding Speed (mm/s)
Al	Al–99.9999 pct	plate H_s: 2.0 W_s: 20.0	Nd:YAG laser	Gaussian	–	0.01	800.0	0.5	0.0
Al-alloy 5182	Al–4.2 pct Mg	plate W_s: 35.0 L_s: 150.0 H_s: 1.0	Nd:YAG	Gaussian	helium at 1.57×10^{-3}	0.012	1600.0 2510.0	0.31 0.42	105.8 105.8
Ga	Ga–99.9999 pct	disc D_s: 25.0 H_s: 10.0	CO_2 laser with	Gaussian	argon	240.0	7.5 7.5 15.0 15.0	2.95 0.75 2.95 0.75	0.0 0.0 0.0 0.0
$NaNO_3$	99.9 pct	plate W_s: 100.0 L_s: 100.0 H_s: 20.0	CO_2 laser	Gaussian	argon	180.0	4.5 12.4 12.4 16.5 16.5	1.60 2.95 0.75 2.95 0.75	0.0 0.0 0.0 0.0 0.0
High speed steel	C–0.88 pct, Cr–3.8 pct, W–6.38 pct, Mo–4.87 pct, V–1.8 pct, Co–4.57 pct, Fe–balance	disc D_s: 30.0 H_s: 15.0	CO_2 laser with	Top hat	argon at 3.33×10^{-4}	5.0	1900.0 5200.0	1.4 1.4	0.0 0.0
Pure iron	–	disc D_s: 25.0 H_s: 1.0	CO_2 laser	Gaussian	argon	0.5	500.0	0.127	0.0
Titanium	Ti–99.7 pct	disc D_s: 25.0 H_s: 1.2	CO_2 laser	Gaussian	argon	0.5	500.0	0.127	0.0

*H_s–specimen thickness, W_s–width of the specimen, L_s–length of the specimen, and D_s–diameter of the disc-shaped specimen.

Steel has a relatively low thermal diffusivity ($=3.9 \times 10^{-6}$ m^2/s) and high Pr (~ 0.2). The resulting Pe (~ 40) was sufficiently high at high laser powers and convective heat transfer played an important role in affecting weld pool shape. High convective flow toward the edge of the weld pool created a strong return flow, which made the weld pool aspect ratio much lower than those of gallium and aluminum, as shown in Figure 4(b). For $NaNO_3$, which is characterized by very high Pr ($=9.15$) and very low thermal diffusivity ($=1.7 \times 10^{-7}$ m^2/s), the calculated values of Pe were very high (10^3 to 10^4). As a result, heat was transported primarily by convection from the center of the weld pool to the edge. With the increase in laser power and decrease in beam radius, the convection became so strong that the fluid rushed towards the edge of the pool and strong return flow from the edge made the periphery deeper than the center, as can be observed from Figure 5(b).

B. *Weld Pool Size and Dimensionless Numbers*

The weld pool geometry in gallium, pure aluminum, aluminum alloy 5182, pure iron, steel, titanium, and sodium nitrate under various welding conditions provides a basis for seeking a correlation among dimensionless numbers that allow determination of weld cross-sectional area from welding parameters and material properties for low speed and laser spot welds. By dimensional analysis, two dimensionless numbers were defined, which are related to each other.

$$\text{Dimensionless cross-sectional area (DA)} = \frac{H_m A}{\alpha_l^2} \quad [4]$$

$$\text{Dimensionless heat input (DH)} = \frac{H_m^{1/2} Q t}{\alpha_l^3 \rho \text{Pr}} \quad [5]$$

where A is the cross-sectional area of the weld pool, Q is the rate of heat absorption, t is the irradiation time, H_m is the enthalpy change per unit mass for heating from room temperature to liquid state at the melting point, α_l is thermal diffusivity of liquid metal at melting point, and Pr is the Prandtl number. It should be noted that spot weld dimensions depend on the duration of irradiation. In industrial practice, laser spot welding operations do not reach quasi-steady state and the variable t represents the irradiation time. However, if laboratory spot welding experiments are conducted for an extended time for gaining better insight, the variable t may have a maximum value. This maximum value is the time after which the spot size does not change, *i.e.*, after the weld reaches quasi-steady state. For low speed welds, the irradiation time is taken as the ratio of the width of the pool and welding velocity.

The correlation between dimensionless heat input and dimensionless area is shown in Figure 7 and can be expressed as

$$\text{DA} = 1.5 \times 10^{-4} \text{DH}^{0.98} \quad [6]$$

where, DA and DH are dimensionless area and dimensionless heat input respectively. The correlation coefficient

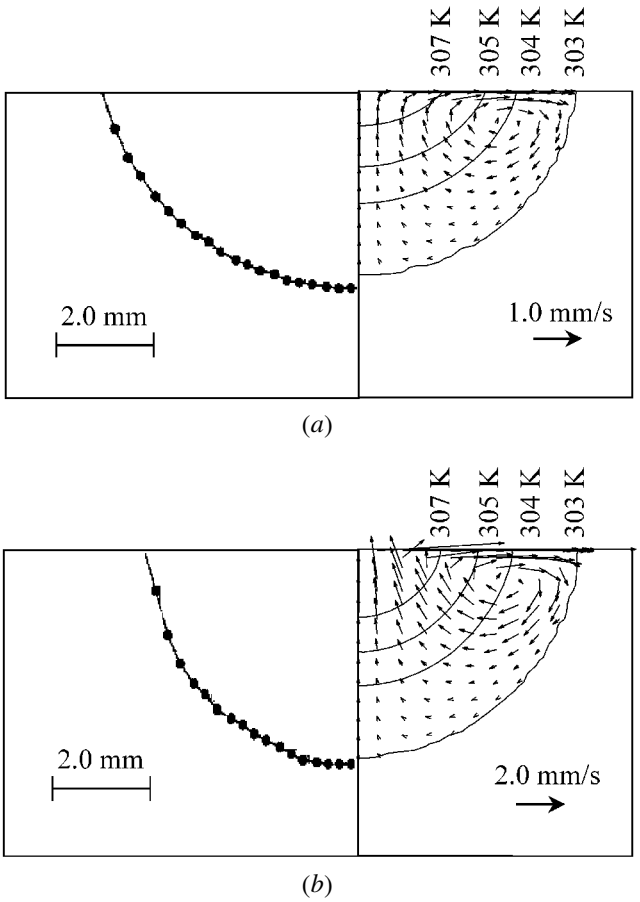

Fig. 2–Comparison of the experimental [7] and predicted spot weld pool geometry in pure gallium at 7.4 W laser power and (*a*) 5.9 mm and (*b*) 1.5 mm beam diameters.

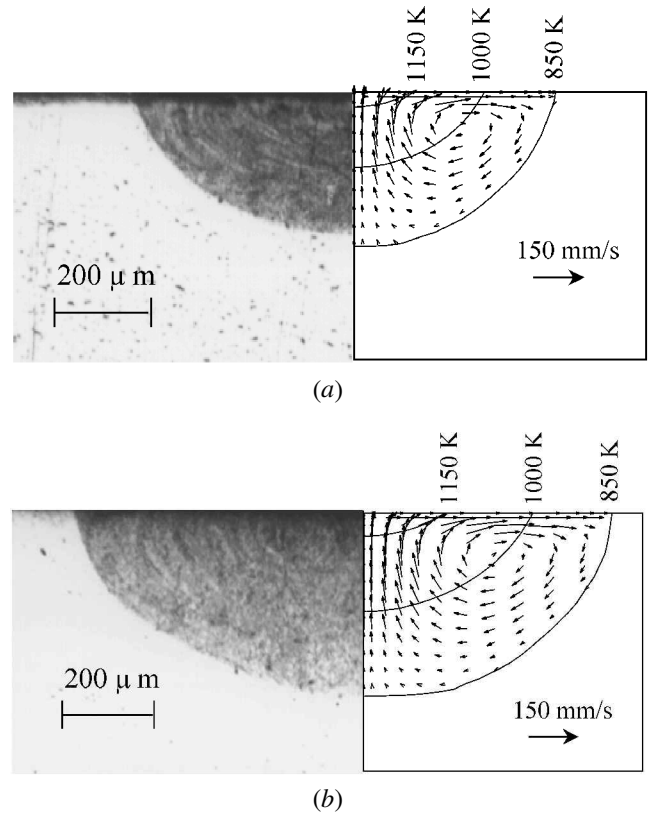

Fig. 3–Experimental [11] and calculated weld pool cross sections for aluminum alloy 5182 at (*a*) 1.5 kW and (*b*) 3.0 kW laser powers, 105.8 mm/s welding speed, and laser beam focused 1.5 mm above the specimen surface.

for the data fit between Eq. [6], and the data was 0.99. It can be observed from Figure 7 that different ranges of dimensionless heat input and dimensionless area were obtained for different materials. Sodium nitrate ($NaNO_3$), which has a very low thermal diffusivity, has a high range of dimensionless heat input and dimensionless area. Aluminum, with its high thermal diffusivity, takes up the lower range of dimensionless heat input and dimensionless area, and the other materials fall between $NaNO_3$ and aluminum. The cross-sectional area of the weld pool can be calculated for laser spot-welds and laser welds at low welding speeds with the help of the dimensionless correlation indicated in Eq. [6].

IV. SUMMARY AND CONCLUSIONS

Computer models of heat transfer and fluid flow were used for the calculation of weld pool geometry in gallium, pure aluminum, aluminum alloy 5182, pure iron, steel, titanium, and sodium nitrate under various welding conditions. The predicted weld pool geometry for various materials under different welding conditions was compared with the independent experimental results. Good agreement was achieved between the computed and the experimental results in each case.

Pe and Ma numbers were found to be important in determining the weld pool shape. A relationship was developed between these two numbers for all materials and welding conditions considered. For a given material, Ma and Pe increased with the increase in input laser power and decrease in beam radius. It was found that for high Pr materials, such as sodium nitrate, the Pe was very high (10^3 to 10^4), and the high value of Pe made the weld pool wide and shallow. For low Pr number materials, such as aluminum alloy 5182, the Pe when calculated using the average velocity in the weld pool was found to be low (<1), and the resulting weld pool was narrow and deep.

A dimensionless correlation is proposed to relate the cross-sectional area of the weld pool with the welding parameters and physical properties of the materials. Using this correlation, the cross-sectional area of the weld pool for low speed and laser spot welds can be predicted without using any heat transfer and fluid flow model.

ACKNOWLEDGMENTS

The present study was supported by the Division of Materials Sciences, Office of Basic Energy Sciences, the United States Department of Energy, under Grant No. DE-FG02-84ER45158. The authors thank Mr. P.W. Fuerschbach for his comments.

LIST OF SYMBOLS

A	cross-sectional area of the weld pool (m^2)
C_{ps}	specific heat of solid (J/kg K, which may also

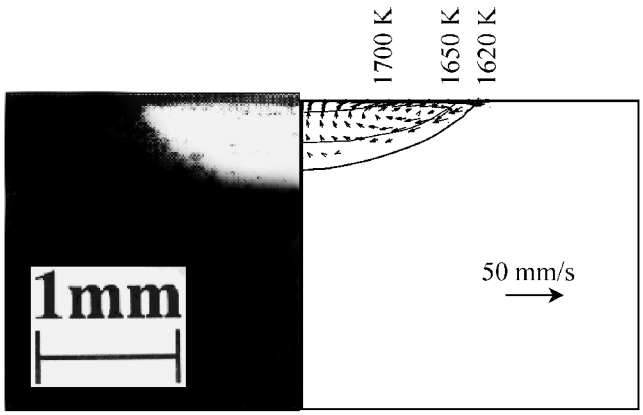

(*a*)

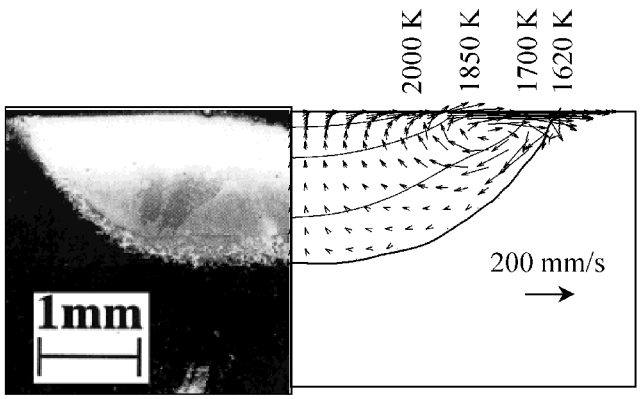

(*b*)

Fig. 4–Comparison of the experimental [12] and predicted spot weld pool geometry in high speed steel for (*a*) 1900 W and (*b*) 5200 W laser powers and 5 s irradiation time.

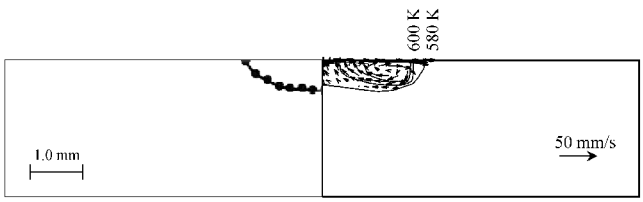

(*a*)

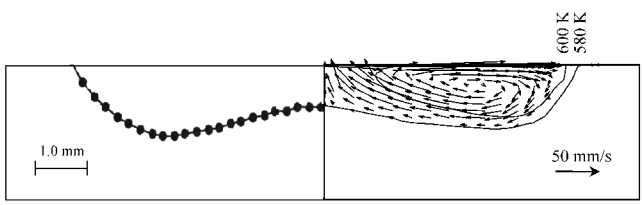

(*b*)

Fig. 5–Comparison of the experimental [7] and predicted spot weld pool geometry in sodium nitrate for the following laser powers and beam diameters: (*a*) 4.5 W, 3.2 mm; and (*b*) 7.5 W, 1.5 mm.

be written as m^2/s^2 K)

C_{pl} specific heat of liquid (J/kg K, which may also be written as m^2/s^2 K)

D depth of the weld pool (m)

DA dimensionless cross-sectional area

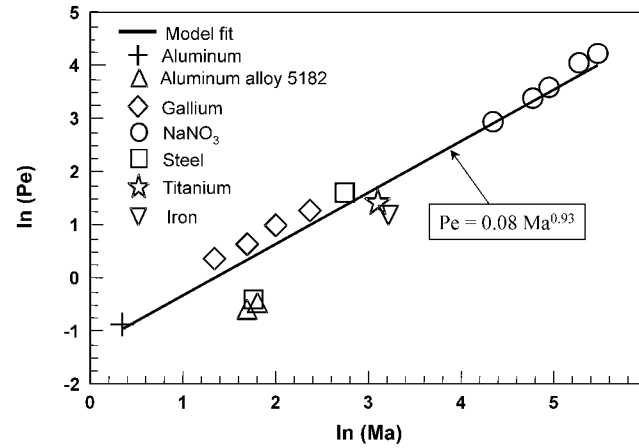

Fig. 6–Relationship between Ma and Pe for different materials and welding conditions.

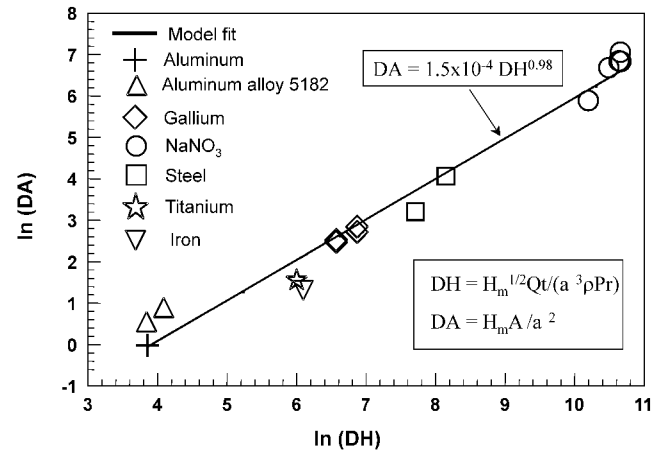

Fig. 7–Correlation between dimensionless cross-sectional area and dimensionless heat input for spot and low speed laser welds.

DH dimensionless heat input

$d\gamma/dT$ temperature coefficient of the surface tension (N/m K, which may also be written as kg/s^2 K)

D_s diameter of disc-shaped specimen (m)

H_f enthalpy of fusion (J/kg, which may also be written as m^2/s^2)

H_m enthalpy of liquid at melting point (J/kg, which may also be written as m^2/s^2)

H_s specimen thickness (m)

K_s thermal conductivity of solid (J/m s K, which may also be written as kg m/s^3 K)

K_l thermal conductivity of liquid (J/m s K, which may also be written as kg m/s^3 K)

L_s length of specimen (m)

Ma Marangoni number

Pe Peclet number

Pr Prandtl number

Q rate of heat absorption (J/s, which may also be expressed as kg/m^2 s^3)

t irradiation time or the time necessary to reach quasi-steady-state size of the weld pool (s)

T_m melting point (K)

V_{max} calculated maximum surface velocity (m/s)

W width of the weld pool (m)

W_s	width of the specimen (m)
α_s	thermal diffusivity of solid (m^2/s)
α_l	thermal diffusivity of liquid (m^2/s)
ΔT	temperature drop from the center to the edge of the weld pool (K)
μ	viscosity (kg/m s)
ν	kinematic viscosity (m^2/s)
ρ	density (kg/m^3)

REFERENCES

1. C.L. Chan, J. Mazumder, and M.M. Chen: *Metall. Trans. A*, 1984, vol. 15A, pp. 2175-84.
2. C.L. Chan, J. Mazumder, and M.M. Chen: *Mater. Sci. Technol.*, 1987, vol. 3, pp. 306-11.
3. K. Mundra, T. DebRoy, and K.M. Kelkar: *Num. Heat Transfer A*, 1996, vol. 29, pp. 115-29.
4. S. Kou and D.K. Sun: *Metall. Trans. A*, 1985, vol. 16A, pp. 203-13.
5. T. Zacharia, S.A. David, J.M. Vitek, and T. DebRoy: *Weld. J.*, 1989, vol. 68 (12), pp. 499-509.
6. S. Kou and Y.H. Wang: *Metall. Trans. A*, 1986, vol. 17A, pp. 2265-70.
7. C. Limmaneevichitr and S. Kou: *Welding J.*, 2000, vol. 79 (8), pp. 231s-237s.
8. P.F. Mendez and T.W. Eager: in *Trends in Welding Research*, J.M. Vitek, S.A. David, J.A. Johnson, H.B. Smartt, and T. DebRoy, eds., ASM INTERNATIONAL, Materials Park, OH, 1998, pp. 13-18.
9. P.W. Fuerschbach: *Welding J.*, 1996, vol. 75 (1), pp. 24s-34s.
10. P.W. Fuerschbach: in *Trends in Welding Research*, H.B. Smartt, J.A. Johnson, and S.A. David, eds., ASM INTERNATIONAL, Materials Park, OH, 1996, pp. 493-97.
11. H. Zhao and T. DebRoy: *Metall. Mater. Trans. B*, 2001, vol. 32B, pp. 163-72.
12. W. Pitscheneder, T. DebRoy, K. Mundra, and R. Ebner: *Welding J.*, 1996, vol. 75 (3), pp. 71s-80s.
13. C. Limmaneevichitr and S. Kou: *Welding J.*, 2000, vol. 79 (5), pp. 126s-135s.
14. E.A. Brandes: *Smithells Metals Reference Book*, 6th ed., in association with Fulmer Research Institute Ltd., Butterworth and Co., London, 1983.
15. E.J. Michaud, D.C. Weckman, and H.W. Kerr: *Int. Congr. on Applications of Lasers and Electro-Optics (ICALEO '94)*, Proc. Conf. on Laser Materials Processing, Oct. 17±20, 1994, Orlando, FL, T. Dwayne McCay, A. Matsunawa, and H. Hůgel, eds. Laser Institute of America, Orlando, FL, 1994, pp. 461-70.
16. S. Basu and T. DebRoy: *J. Appl. Phys.*, 1992, vol. 72 (8), pp. 3317-22.